Calcium-Binding Site β2, Adjacent to the "b" Polymerization Site, Modulates Lateral Aggregation of Protofibrils during Fibrin Polymerization[†,‡]

Michael S. Kostelansky,[⊥] Karim C. Lounes,[||] Li Fang Ping,[||] Sarah K. Dickerson,[||] Oleg V. Gorkun,[||] and Susan T. Lord*[,||,⊥]

Department of Chemistry and Department of Pathology and Laboratory Medicine, University of North Carolina, Chapel Hill, North Carolina 27599

Received November 8, 2003; Revised Manuscript Received December 20, 2003

ABSTRACT: Structural analysis of recombinant fibrinogen fragment D revealed that the calcium-binding site (β2-site) composed of residues BβAsp261, BβAsp398, BβGly263, and γGlu132 is modulated by the "B:b" interaction. To determine the β2-site's role in polymerization, we engineered variant fibrinogen γE132A in which calcium binding to the β2-site was disrupted by replacing glutamic acid at γ132 with alanine. We compared polymerization of γE132A to normal fibrinogen as a function of calcium concentration. Polymerization of γE132A at concentrations of calcium ≤1 mM exhibited an uncharacteristic 2−3-fold increase in lateral aggregation and fiber thickness compared to normal fibrinogen, while polymerization of variant and normal were indistinguishable at 10 mM calcium. These results suggest that the β2-site controls the extent of lateral aggregation. That is, when the calcium anchor (β2-site) is eliminated before "B:b" interactions occur then lateral aggregation is enhanced. We solved structures of fragment D of γE132A fibrinogen (rfD-γE132A) with and without Gly-His-Arg-Pro-amide (GHRPam) and found no change to the global structure. X-ray diffraction data showed GHRPam binding in the "a" and "b" polymerization sites and that calcium could still bind to the β2-site of γE132A fibrinogen at 70 mM calcium. We found that the γ2 calcium-binding site (in loop γ294−301) did not have calcium bound in the structure of fragment D of γE132A fibrinogen with GHRPam bound (rfD-γE132A+GH). Analysis of structures rfD-γE132A+GH and rfD-BβD398A+GH indicated that differences in calcium occupation of the γ2-site resulted from minor conformational changes provoked by crystal packing and GHRPam binding to the "a" site did not directly modulate calcium binding to this site.

Fibrinogen, a soluble plasma protein, is composed of six polypeptide chains, (Aα, Bβ, γ)$_2$. These six polypeptide chains, held together by 29 disulfide bonds, fold to form a 340 kDa trinodular protein molecule. The central nodule of the fibrinogen molecule, called E, is flanked by two terminal nodules designated D (*1*, *2*). Each D nodule links to the central E nodule by a coiled coil connector (*3*). The amino termini of all six polypeptide chains originate in the E nodule. The carboxyl termini of the Bβ- and γ-chains extend outward from the E nodule and fold into two independent modules in the D nodule. The carboxyl termini of the Aα chains (αC domains) have been shown to extend freely in solution or participate in noncovalent interactions with the E nodule (*4*).

Fibrinogen is transformed to insoluble fibrin when thrombin, generated at the end of the coagulation cascade, cleaves fibrinopeptides A and B (FpA and FpB)[1] from the amino termini of the Aα- and Bβ-chains, respectively. The newly exposed sequences at the amino termini of the α-chains compose the polymerization sites "A" (GPRV), while the amino termini of the β-chains compose the polymerization sites "B" (GHRP) (*5*−*7*). These sites can interact with complimentary binding sites, called "a" and "b", which reside in the γ- and β-modules, respectively (*8*). Upon cleavage of FpA, fibrin monomers interact with one another through interactions of "A" with "a" ("A:a") to form double-stranded, half-staggered protofibrils. Protofibrils grow to a critical length at which time they begin to laterally aggregate to form thick branching fibers (*9*). FpB cleavage occurs predominantly during protofibril formation, which allows interactions of polymerization site "B" with its complementary site "b". The "B:b" interaction has been shown to enhance lateral aggregation (*10*). The significance of the "B:b" interaction to polymerization remains debatable, because fibrinogen can form a clot when only FpA is cleaved and presumably only "A:a" interactions occur (*11*). Experiments with recombinant

[†] This work was supported by National Institutes of Health Grant HL 31048 (S.T.L.).

[‡] The atomic coordinates have been deposited in the Protein Data Bank (www.rcsb.org) under the access codes 1RF0 (rfD-γE132A) and 1RF1 (rfD-γE132A+GH).

* Corresponding Author: Susan T. Lord, Ph.D, University of North Carolina at Chapel Hill, Department of Pathology and Laboratory Medicine, CB #7525, Brinkhous-Bullitt Building room 822, Chapel Hill, NC 27599-7525. Phone: (919) 966−3548. Fax: (919) 966-6718. E-mail: stl@med.unc.edu.

[⊥] Department of Chemistry.

[||] Department of Pathology and Laboratory Medicine.

[1] Abbreviations: rfD, recombinant fibrinogen fragment D; rfD-BOTH, recombinant fibrinogen fragment D with GPRPam and GHRPam bound; rfD-γE132A, fragment D of γE132A fibrinogen; rfD-γE132A+GH, fragment D of γE132A fibrinogen with GHRPam bound; GPRPam, Gly-Pro-Arg-Pro-amide; GHRPam, Gly-His-Arg-Pro-amide; FpA, fibrinopeptide A; FpB, fibrinopeptide B; HEPES, *N*-(hydroxyethyl)piperazine-*N*′-(2-ethanesulfonic acid); GPRPAA, Gly-Pro-Arg-Pro-Ala-Ala; EDTA, ethylenediaminetetraacetic acid.

10.1021/bi0359978 CCC: $27.50
Published on Web 02/10/2004

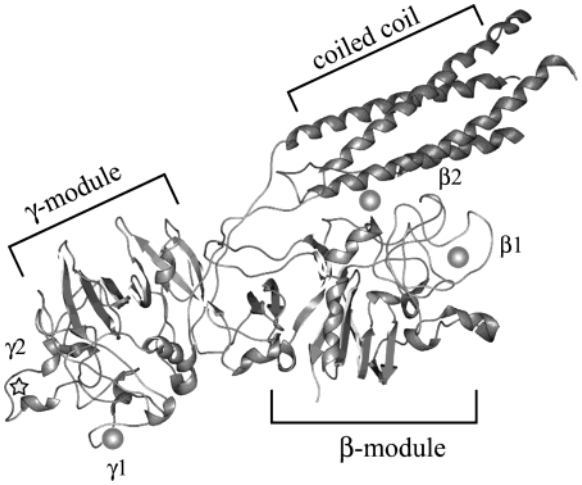

FIGURE 1: Location of the calcium atoms bound in calcium-binding sites in the fibrinogen fragment D molecule. The ribbon diagram represents the structure of recombinant fibrinogen fragment D. The calcium-binding sites γ1, β1, and β2 are shown as spheres; the γ2 site is shown as a star. To identify the residues that make up these calcium-binding sites, see text.

variant fibrinogens with impaired "A:a" interactions suggest that "B:b" interactions may have a role in protofibril formation (*12*). As described in the preceding manuscript, analysis of recombinant fibrinogens with severely impaired "B:b" interactions also points to the importance of "B:b" interactions to normal polymerization.

Many aspects of fibrinogen function are modulated by calcium ions. Calcium ions promote polymerization, influence activation of Factor XIII, and affect fibrinolysis by changing plasmin cleavage of fibrinogen (*13*−*15*). Data from X-ray crystal structures of recombinant γ-module, plasma fragment D, plasma cross-linked fragment D−D, and recombinant fragment D have shown the presence of four possible calcium sites in the D nodule of fibrinogen, Figure 1 (*8*, *16*−*19*). We have designated these sites as γ1, γ2, β1, and β2. The primary γ-module calcium site, γ1, is the well-characterized "high-affinity calcium-binding site" (*16*, *17*). It is composed of the side chains of residues γAsp318 and γAsp320 and the backbone carbonyls of γPhe322, and γGly324. The γ2-site is located opposite the γ1-site and has been reported to appear as a result of GHRPam ("B" site peptide analog) binding in the "a" polymerization site (*18*). The side chains of residues γAsp294 and γAsp301 and backbone carbonyls of residues γGly296 and γAsp298 comprise the γ2 calcium-binding site. The remaining two calcium-binding sites reside near and in the β-module of fibrinogen. The β1-site is located at a homologous position to that of the γ1-site and includes the side chains of residues BβAsp381 and BβAsp383 and the backbone carbonyl of BβTrp385. The β2 calcium-binding site is located adjacent to the "b" polymerization site and encompasses the side chains of residues BβAsp261, BβAsp398, and γGlu132 and backbone carbonyl of BβGly263. Structural data have shown that the β2-site, which serves as an anchor between the coiled coil connector and the β-module, Figure 1, is modulated by the binding of GHRPam. That is, when GHRP is bound, the calcium link is abolished thus permitting potential movement of the β-module (*19*).

To further investigate the structure of the β2 calcium-binding site and understand its role in polymerization, we engineered a recombinant variant fibrinogen, γE132A, with alanine substituted for a glutamic acid residue at position 132 of the γ-chain. This residue, γGlu132, is involved in coordinating calcium at the β2-site. We hypothesized that the introduced mutation would remove one calcium coordinate thereby weakening or eliminating the β2-site. To determine the effect of the β2-site on polymerization, we performed fibrinogen polymerization as a function of calcium concentration. In addition, we also used X-ray crystallography to solve structures of fragment D from γE132A alone (rfD-γE132A) at 2.8 Å and in the presence of GHRPam (rfD-γE132A+GH) at 2.5 Å to examine the consequences of this substitution on the structure and integrity of the β2 calcium-binding site and the "b" polymerization site.

MATERIALS AND METHODS

Chemicals were reagent grade and, unless specified, were purchased from Sigma (St. Louis, MO). The peptide GHRPam was synthesized by the Protein Chemistry Laboratory of the University of North Carolina (Chapel Hill, NC). Human thrombin was purchased from Enzyme Research Laboratories, Inc. (South Bend, IN). The monoclonal antibody IF-1 was purchased from Iatron Corp. (Tokyo, Japan). Cyanogen bromide-activated Sepharose 4B was purchased from Amersham Biosciences (Piscataway, NJ). Normal recombinant fibrinogen media was obtained from the National Cell Culture Center (Minneapolis, MN).

Synthesis of Fibrinogen γE132A. The expression vector employed in our study, pMLP-γ, contains the cDNA for the human γ-chain of fibrinogen and has been described previously (*20*). The glutamic acid residue at position γ132 was replaced with an alanine by way of oligo-directed mutagenesis, using the Transformer TM site-directed mutagenesis kit (Clontech, Palo Alto, CA) based on a method outlined by Deng et al. (*21*). The primer used to construct the substituted vector was 5′GCCCAGCTTGCAGCACAGTGCC3′. Sequencing of the mutated cDNA was performed to ensure that only the desired changes were introduced. Synthesis of the variant fibrinogen was completed as described (*22*). Briefly, the mutated pMLP-γ vector and selection vector pMSV-His were cotransfected into Chinese hamster ovary cells (CHO cells) expressing the human fibrinogen polypeptide chains Aα and Bβ. Individual clones secreting high amounts of fibrinogen as determined by an enzyme-linked immunosorbent assay were selected for large-scale protein expression. Protein production was carried out in roller bottles in serum-free medium containing aprotinin. The medium containing secreted protein was harvested periodically, phenylmethylsulfonyl fluoride was added, and the medium was then stored at −20 °C.

Purification of Recombinant Fibrinogen. Both normal and γE132A fibrinogens were isolated from the medium by a two-step method outlined previously (*23*). In brief, the first step, ammonium sulfate precipitation, concentrated the fibrinogen, while the second step, immunoaffinity chromatography using the calcium-dependent, fibrinogen-specific antibody IF-1 linked to Sepharose 4B, was used to isolate fibrinogen. Elution of fibrinogen was achieved by using buffer containing 5 mM EDTA. The purified fibrinogens were dialyzed against 20 mM HEPES, pH 7.4, and 150 mM

NaCl (HBS) with 1mM $CaCl_2$ followed by extensive dialysis against HBS. Aliquots of protein were stored at −70 °C until use. Purity and proper polypeptide chain composition of the recombinant fibrinogens was confirmed by SDS−PAGE analysis under reduced and nonreduced conditions.

Fibrinopeptide Release. Fibrinopeptide release assays were performed as described (*22*, *24*). Briefly, fibrinogen (0.1 mg/mL) in HBS was incubated with human thrombin (0.005 NIH unit/mL) at ambient temperature. At specific intervals, reactions were stopped by boiling, the samples were centrifuged, and the supernatants were analyzed by reverse-phase HPLC to determine the amounts of FpA and FpB present. Statistical significance of the data was determined by using unpaired *t*-tests. A value was considered significant if *p* was less than 0.05.

Thrombin-Catalyzed Polymerization. Polymerization of normal and γE132A fibrinogen catalyzed by thrombin at ambient temperature was monitored by following the rise in turbidity at 350 nm in a SpectraMax-340PC microplate reader (Molecular Devices, Sunnyvale, CA) essentially as described (*25*). The reactions were carried out in HBS buffer containing 1 μM, 1 mM, or 10 mM $CaCl_2$. Sample preparation included overnight dialysis of the fibrinogens against HBS containing the above-mentioned concentrations of calcium chloride and dilution of human α-thrombin in HBS immediately before use. Reactions were initiated by adding 10 μL of thrombin (1 NIH unit/mL) with a multichannel pipet to wells containing 90 μL of fibrinogen (0.22 mg/mL). Immediately upon addition of thrombin, the wells were mixed for 5 s with the automix function of the instrument, and the absorbance at 350 nm was read every 24 s for 3 h. A minimum of four experiments was carried out for each reaction condition.

Polymerization data were analyzed by measuring the lag time, V_{max}, and final absorbance for each reaction, as described (*26*). The lag time, which correlates with the rate of protofibril formation, was defined as the time elapsed from the addition of thrombin until an increase in turbidity was seen. The V_{max} was the slope at the steepest portion of the polymerization curve and is related to the rate of lateral aggregation of protofibrils. The final absorbance, a quantity representing the thickness of fibers, was measured as the absorbance at 350 nm at 60 min into the polymerization reaction. Data for normal fibrinogen and variant fibrinogen, γE132A, were compared to determine statistical significance using unpaired *t*-tests. A difference was considered significant if the *p* value was less than 0.05.

Preparation of Fragment D from γE132A Fibrinogen. Seven milligrams of γE132A fibrinogen (final concentration of 0.66 mg/mL) in HBS with 20 mM $CaCl_2$ was digested to make fragment D (rfD-γE132A), as described (*19*). Briefly, the digest reaction was initiated by adding 100 μL of immobilized TPCK trypsin (Pierce, Rockford, IL), incubation continued over a period of days and was monitored for progress by SDS−PAGE. When only rfD-γE132A and the E fragment bands were visible on SDS−PAGE (data not shown), the digest was stopped by removing the trypsin-coated beads by filtering through a 0.22 μm syringe fitting filter (Costar, Corning, NY). The digested protein was stored at −70 °C.

Fragment D of γE132A fibrinogen was purified by peptide affinity chromatography based on a method described by Everse et al. (*27*) with slight modification (*19*). In brief, the peptide GPRPAA was synthesized by solid-phase methods and deblocked while remaining covalently linked to a polymeric resin, which served as the affinity matrix (personal communication, Dr. David Klapper, UNC, Chapel Hill, NC). All seven milligrams of digested γE132A fibrinogen were loaded onto a 2 mL GPRPAA affinity column equilibrated with HBS containing 20 mM $CaCl_2$ (loading buffer) at a flow rate of 10 mL/hr. The column was washed with loading buffer and HBS with 0.5 M NaBr until no material absorbing at 280 nm was eluting from the column. The rfD-γE132A was eluted with 1 M NaBr, 50 mM sodium acetate, pH 5.3. Fractions containing rfD-γE132A were pooled, dialyzed against 50 mM Tris, pH 7.4, and concentrated with a centrifugal filter device (10 kDa MW cutoff, Millipore Corp., Billerica, MA). The protein was stored at 4 °C.

Crystallization of γE132A Recombinant Fragment D. Crystals of rfD-γE132A were obtained by sitting-drop vapor diffusion at 4 °C. Conditions were screened near those previously reported (*8*, *17*−*19*, *27*). For rfD-γE132A, 5 μL of 12 mg/mL protein in 50 mM Tris, pH 7.4, was mixed with an equal volume of well solution containing 50 mM Tris, pH 8.5, 2 mM NaN_3, 70 mM $CaCl_2$, and 14−15% PEG 3350. A method of streak seeding from crystals of normal rfD was employed to maximize rfD-γE132A crystal growth. In general, these crystals grew in a few days time as small clusters of plates. Single crystals for X-ray diffraction were removed from these clusters by gentle prodding with a crystal loop.

Crystals of rfD-γE132A were also grown in the presence of GHRPam (rfD-γE132A+GH). Sitting drops at 4 °C were prepared by mixing 5 μL of protein solution containing rfD-γE132A at 10 mg/mL, 50 mM Tris, pH 7.4, and 2 mM GHRPam with 5 μL of well solution consisting of 50 mM Tris, pH 8.5, 2 mM NaN_3, 12.5 mM $CaCl_2$, and 9−10% PEG 3350. Crystals appeared in days, and again seeding from crystals of normal rfD maximized growth of diffraction-quality crystals.

X-ray Data Collection. X-ray diffraction data for both rfD-γE132A and rfD-γE132A+GH were collected at 100 K at the Stanford Synchrotron Radiation Laboratory (SSRL), beamline 9-1. In preparation for low-temperature data collection, crystals were cryoprotected in a solution composed of the crystallant plus 20% glycerol. The crystals were mounted in loops, flash frozen with liquid nitrogen, and stored in liquid nitrogen until used. Diffraction data from both crystals were processed using DENZO and SCALEPACK (*28*).

Structure Determination. The unit cells of rfD-γE132A and rfD-γE132A+GH (Table 1) were isomorphous to those found for normal recombinant fragment D (rfD, PDB id = 1LT9) and normal recombinant fragment D in the presence of two peptide ligands (rfD-BOTH, PDB id = 1LTJ) (*19*). Therefore both structures, rfD-γE132A and rfD-γE132A+GH, were refined by rigid-body minimization followed by simulated annealing using 1LT9 and 1LTJ as starting models, respectively. CNS (*29*) was used for the refinement and an alanine replaced the glutamic acid at position γ132 in the starting models.

Structures rfD-γE132A and rfD-γE132A+GH were further refined via CNS. The computational refinement process used least-squares minimization, simulated annealing, and individual temperature factor refinement including an overall

Table 1: X-ray Crystallography Data and Refinement Statistics

	rfD-γE132A	rfD-γE132A+GH
resolution (Å)	18−2.8	18−2.53
space group	$P2_12_12_1$	$P2_12_12_1$
cell constants (Å)	$a = 88.4$	$a = 89.7$
	$b = 94.9$	$b = 94.7$
	$c = 227.6$	$c = 228.2$
molecules/asymmetric unit	2	2
total observations	186713	264892
unique reflections	46581	66025
mean redundancy	4.0	4.0
R_{sym}[a] (%; highest shell)	11.0 (40.8)	9.0 (35.9)
completeness (%; highest shell)	99.5 (99.6)	99.9 (100)
mean I/σ (highest shell)	13.0 (3.4)	13.8 (4.0)
R_{cryst}[b] (%)	23.3	23.4
R_{free}[c] (%)	28.6	28.1
RMSD bond lengths (Å)	0.0068	0.0064
RMSD bond angles (deg)	1.24	1.24
average *B*-factor	40.0	38.5
number of model atoms	10778	10934
number solvent sites	116	248

[a] $R_{sym} = \sum|I - \langle I\rangle|$ where I is the observed intensity and $\langle I\rangle$ is the average intensity of multiple symmetry-related observations of that reflection. [b] $R_{cryst} = \sum||F_{obs}| - |F_{calc}||/\sum|F_{obs}|$, where F_{obs} and F_{calc} are the observed and calculated structure factors, respectively. [c] $R_{free} = \sum||F_{obs}| - |F_{calc}||/\sum|F_{obs}|$ for 5% of the data withheld from structural refinement.

anisotropic B-factor and bulk solvent correction (*29*). Before refinement of either structure, 5% of the observed data was set aside for cross-validation using the free *R*-factor statistic (*30*). After the initial round of refinement, manual fitting of both structures was carried out using the software program O (*31*) and σA-weighted $|2F_o - F_c|$ and $|F_o - F_c|$ electron density maps (*32*). Cycles of manual fitting and refinement were performed while following the working *R*-factor and free *R*-factor statistics to assess the progress of rebuilding. In the final stage of refinement, 116 and 248 solvent molecules were added to the structures rfD-γE132A and rfD-γE132A+GH, respectively, and cis peptide bonds were introduced at positions Bβ407 and γ339. The *R*-factor, 24.7%, and free *R*-factor, 29.6%, in the rfD-γE132A structure improved to 23.3% and 28.6%, respectively, after the changes. Similarly in the rfD-γE132A+GH structure, the *R*-factor dropped from 25.7% to 23.4% and the free *R*-factor decreased from 30.4% to 28.1% after the changes were introduced.

RESULTS

Characterization of γE132A. We synthesized the variant fibrinogen, γE132A, and purified it from cell culture medium by a two-step precipitation/immunoaffinity chromatography procedure as described in the Materials and Methods. The variant was analyzed by SDS−PAGE under nonreduced conditions and found to be pure and assembled into a 340 kDa molecule, similar to normal recombinant fibrinogen, Figure 2A. Under reduced conditions, SDS−PAGE revealed the expected band pattern corresponding to the three polypeptide chains that compose the fibrinogen molecule, Figure 2B.

Fibrinopeptide Release. We monitored thrombin-catalyzed release of FpA and FpB by measuring the percent of released peptides following their separation by HPLC (data not shown). The specificity constant (k_{cat}/K_m) for FpA was determined to be $(6.6 \pm 0.5) \times 10^6$ M^{-1} s^{-1} for both normal and γE132A fibrinogen, while the specificity constant for FpB was $(3.1 \pm 0.5) \times 10^6$ and $(1.9 \pm 0.5) \times 10^6$ M^{-1} s^{-1} for normal and γE132A fibrinogen, respectively. FpA and FpB specificity constants for both normal and variant γE132A fibrinogen were determined to be statistically similar by way of an unpaired *t*-test (*p* value > 0.05). This result meant that the rate of fibrinopeptide release of both proteins was similar allowing direct comparison of their polymerization profiles.

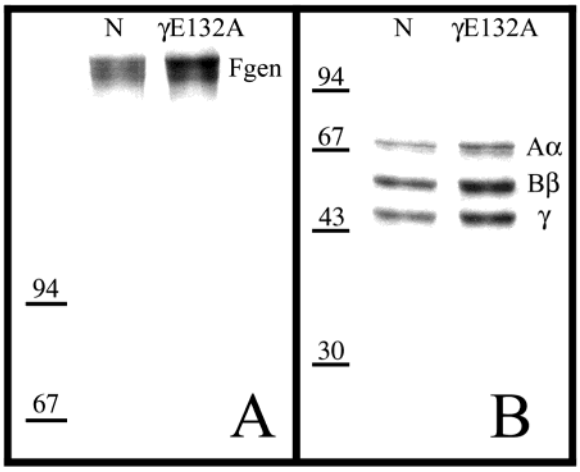

FIGURE 2: SDS−PAGE analysis of γE132A fibrinogen. Panel A shows bands of normal fibrinogen (N) and γE132A fibrinogen (γE132A) run on a 6% SDS−PAGE gel under nonreduced conditions. Panel B shows bands corresponding to the individual polypeptide chains of fibrinogen (Aα-, Bβ-, and γ-chain) of normal fibrinogen (N) and of γE132A fibrinogen (γE132A) run on a 10% SDS−PAGE gel under reduced conditions. Position of molecular weight markers (kDa) are shown on the left in both panels.

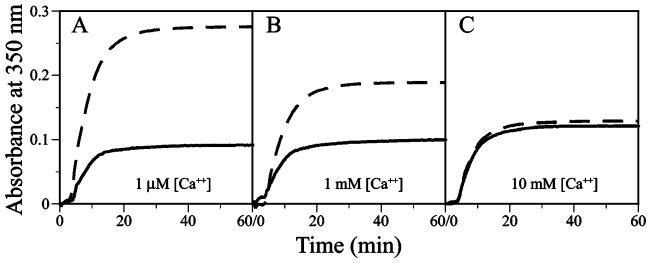

FIGURE 3: Thrombin-catalyzed polymerization of normal and γE132A fibrinogen. Turbidity curves for fibrinogen (0.2 mg/mL) polymerized with thrombin (0.1 U/mL) were monitored at 350 nm with 1 μM (A), 1mM (B), and 10 mM $CaCl_2$ (C). All curves represent averaged data. The solid line represents normal fibrinogen; the broken line represents γE132A fibrinogen.

Polymerization. We monitored thrombin-catalyzed polymerization as the change in absorbance at 350 nm to measure the lag time, which corresponds to protofibril formation. V_{max}, which reflects lateral aggregation, was also determined, and the final absorbance correlated to the extent of lateral aggregation. Our experiments were carried out at three calcium concentrations, 1 μM, 1 mM, and 10 mM, to determine the effect of calcium on the polymerization of fibrinogen γE132A. Representative curves are shown in Figure 3, and average data are presented in Table 2. As shown in Figure 3, the differences in polymerization between normal and variant were quite pronounced at low concentrations of calcium (1 μM and 1mM, Figure 3A,B), while a high calcium concentration (10 mM, Figure 3C) eliminated these differences. At concentrations of $CaCl_2$ less than or

Table 2: Polymerization Parameters for Normal Fibrinogen and γE132A Fibrinogen[a]

	lag time (s)	V_{max} ($\times 10^{-4}$ s^{-1})	final abs at 350 nm[b]
	Normal		
1 μM $CaCl_2$	236 ± 5	1.0 ± 0.2	0.091 ± 0.002
1 mM $CaCl_2$	235 ± 14	0.88 ± 0.1	0.10 ± 0.005
10 mM $CaCl_2$	236 ± 5	1.2 ± 0.2	0.12 ± 0.005
	γE132A		
1 μM $CaCl_2$	219 ± 11	3.0 ± 0.2[c]	0.28 ± 0.002[c]
1 mM $CaCl_2$	264 ± 14	2.2 ± 0.3[c]	0.19 ± 0.006[c]
10 mM $CaCl_2$	264 ± 13	1.6 ± 0.2	0.13 ± 0.006

[a] $n \geq 4$ for each value. [b] Final abs was determined as the absorbance at 350 nm at the 60 min time point of a polymerization reaction. [c] Signifies values found to be statistically different from normal fibrinogen by an unpaired *t*-test.

equal to 1 mM, variant γE132A showed a 2−3-fold increase in V_{max} and final absorbance when compared to normal fibrinogen. In contrast, at 10 mM calcium chloride, the V_{max} and final absorbance values were not statistically different from normal fibrinogen. The lag time for fibrinogen γE132A was not significantly different from normal fibrinogen at any calcium concentration. These data showed that unlike normal fibrinogen, polymerization of γE132A fibrinogen was faster at low calcium concentrations with an increased rate of protofibril assembly and enhanced fiber thickness.

General Structural Features of rfD-γE132A. We crystallized rfD-γE132A with and without GHRPam, a peptide ligand mimicking the "B" polymerization site. The rfD-γE132A and rfD-γE132A+GH structures both had unit cells with approximate dimensions $a = 89$ Å, $b = 95$ Å, and $c = 228$ Å and space group $P2_12_12_1$ (Table 1), similar to the crystals of normal rfD (*19*). The rfD-γE132A+GH structure showed that this variant has a carbohydrate linked to Bβ Gln364 with the added fucose moiety as seen in previously reported rfD structures (*19*). Electron density maps in the rfD-γE132A structure allowed us to visualize additional residues at the N-terminus of the γ-chain in the second molecule in the asymmetric unit beyond those shown in previous models of recombinant fragment D. The newly modeled amino terminus of the γ-chain revealed a crystal-packing contact that included an unwinding α-helix that ended with a hydrogen bond between γTyr96 of one molecule in one asymmetric unit and γAsp272 of the other molecule in another asymmetric unit.

The structures of rfD-γE132A and rfD-γE132A+GH were essentially identical to the structures of rfD and rfD-BOTH, respectively. Alignment of the Cα-atoms of rfD-γE132A with rfD (1LT9) yielded a root-mean-square deviation (RMSD) of 0.41 Å, while the Cα-alignment of rfD-γE132A+GH and rfD-BOTH (1LTJ) resulted in a RMSD of 0.37 Å. The substitution of γGlu132 with alanine was clearly seen in electron density maps of both rfD-γE132A and rfD-γE132A+GH structures. We found that this substitution did not change the local or global structure of fragment D, except for the few interactions that are directly related to residue γGlu132. In particular, alanine at position γ132 did not coordinate with calcium in the β2 calcium-binding site (Figure 4) or form a salt link with residue αLys157 when the β2-site was unoccupied by calcium.

Peptide Binding in rfD-γE132A. The rfD-γE132A+GH crystal data showed GHRPam bound in both the "a" and "b" polymerization sites. These data demonstrated the variant γE132A has a functional "b" polymerization site. Relevant conformational changes such as the movement of residues Bβ Glu397 and Bβ Asp398 toward GHRPam in "b" polymerization site occurred even though the mutation is located in the β2 calcium-binding site, which is in close proximity to the "b" polymerization site, Figure 5. The presence of GHRPam in the "a" polymerization site verified the previously reported findings (*18*, preceding manuscript) in which this peptide was bound in the "a" polymerization site when GPRPam (the "A" site peptide model) was not present.

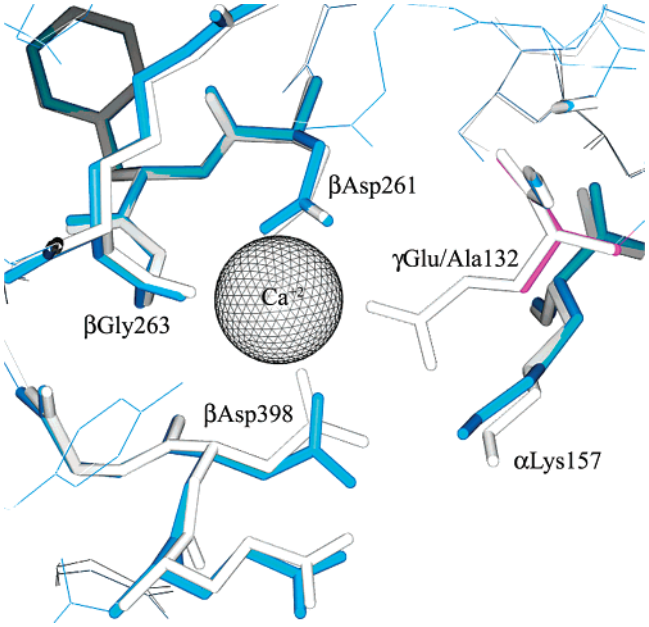

FIGURE 4: Comparison of rfD and rfD-γE132A at the β2 calcium-binding site. The rfD residues corresponding to the rfD structure are shown in gray, while the rfD-γE132A residues are shown in blue with the exception of the substituted alanine in purple. The position of the calcium atom in both structures is represented as a single sphere.

Calcium Binding in rfD-γE132A and rfD-γE132A+GH. The structure of rfD-γE132A, grown at a calcium ion concentration of 70 mM, showed bound calcium ions in three sites, γ1, β1, and β2. Although the substitution at residue γ132 was engineered to disrupt the β2 calcium-binding site by replacing the calcium-coordinating glutamic acid with alanine, the structural data of rfD-γE132A clearly showed a fully occupied β2-site. In fact, as shown in Figure 4, three residues, βAsp261, βGly263, and βAsp398, of the normal four β2-site residues coordinated the calcium ion. It must be noted however that the crystal of rfD-γE132A was grown in the presence of 70 mM calcium, about 35 times the normal plasma calcium concentration. Moreover, because the polymerization data (Figure 3) showed marked differences between 1 mM and 10 mM calcium and nearly normal polymerization at 10 mM calcium, we infer that at physiologically relevant concentrations of calcium the β2 calcium-binding site is significantly less occupied or even completely eliminated. As with normal fibrinogen in the presence of GHRPam, the structure of rfD-γE132A+GH grown at conditions of 12.5 mM calcium showed no calcium bound in the β2-site in the presence of bound GHRPam in the "b" polymerization site.

In contrast to retaining calcium bound to the β2-site in rfD-γE132A at 70 mM calcium concentration, we found no

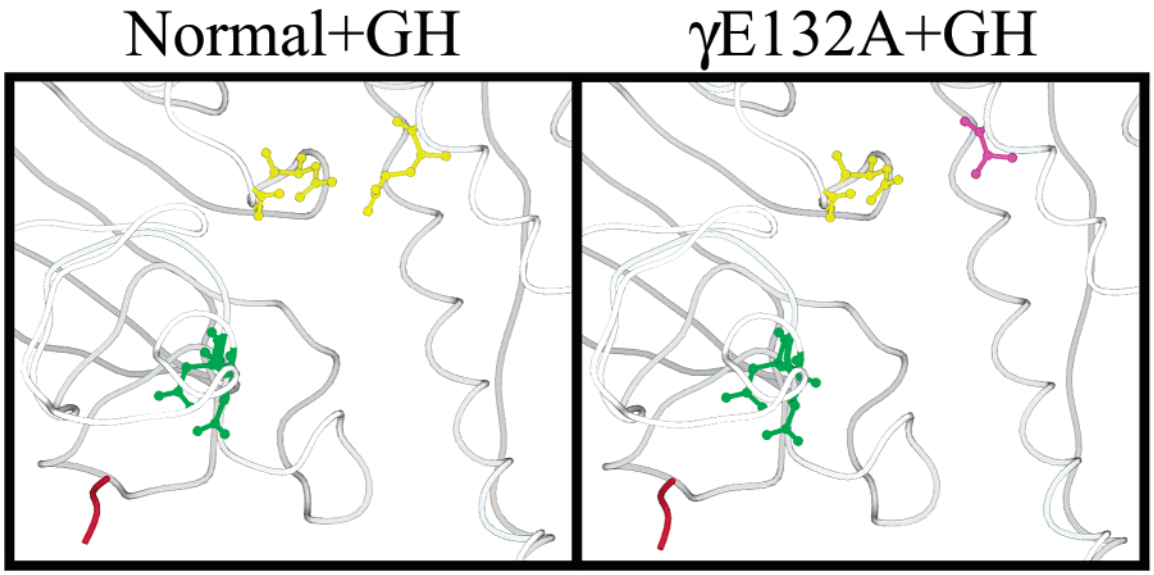

FIGURE 5: GHRPam binding in rfD and rfD-γE132A. Panels compare the "b" polymerization site and nearby β2-site where the γE132A substitution was made in the structures of rfD-BOTH (1LTJ), left, and rfD-γE132A+GH, right. Gray worms represent the protein backbone in both panels. The red worm is the bound peptide, GHRPam, in the "b" polymerization site. Residues BβE397 and BβD398 (green) are highlighted to show their position toward the peptide (red). Residues shown in yellow are the remaining residues that comprised the β2-site where calcium is not bound in either structure. The purple residue is the substituted alanine. Note that both normal and γE132A structures bind GHRPam and the flip of residues BβE397 and BβD398 to interact with the peptide occurs.

calcium bound in the γ2-site in rfD-γE132A+GH grown at 12.5 mM calcium in any of the molecules of the asymmetric unit. The γ2-site was initially identified in plasma fragment D crystallized in the presence of GHRPam and was described as being a function of GHRPam binding to the "a" site (*18*). As shown in Figure 6A, calcium was not bound at the γ2-site in the rfD-γE132A+GH structure, even though GHRPam was bound to the "a" polymerization site. This finding is reminiscent of our finding described in the preceding manuscript with the structure of rfD-βD398A+GH. In this structure, the γ2 calcium-binding site was seen in one (Figure 6B) but not the other (Figure 6C) molecule in the asymmetric unit. Thus, the structure of the variant βD398A in the presence of GHRPam suggested that crystal packing induced minor conformational changes conducive to calcium binding to the γ2-site. The structure of rfD-γE132A+GH now confirms the γ2-site is a result of local changes produced by crystal packing.

DISCUSSION

This paper is the second in a series describing studies that combine the techniques of protein engineering and X-ray crystallography to synthesize and structurally examine functional mutations in fibrinogen. This particular study involved the recombinant variant fibrinogen, γE132A, which was designed to remove the carboxylate side chain of γGlu132 and thus eliminate a coordinating residue in the β2 calcium-binding site. We hypothesized that calcium binding at the β2-site would be impaired or eliminated, in turn revealing the impact of this site on polymerization. The polymerization and structural data support two conclusions: (1) loss of the carboxylate side chain of γE132A impaired calcium binding at the β2-site, thus eliminating the calcium anchor at physiologic concentrations of calcium but not at calcium concentrations of 10 mM or greater, and (2) γE132A fibrinogen retained the ability to support "B:b" interactions, and at physiologic calcium concentrations, its lateral aggregation was enhanced.

Considering the crystallography data of rfD-γE132A, which showed the β2 calcium-binding site was occupied at 70 mM calcium, together with fibrinopeptide release and polymerization data, which showed normal fibrinopeptide release for γE132A but a 2−3-fold increase in the rate of lateral aggregation and fiber thickness compared to normal fibrinogen at ≤1 mM calcium, we conclude that the loss of the side chain carboxylate altered the affinity of the β2-site. Thus, the normal β2-site has an affinity such that calcium is bound and the γE132A variant has an affinity such that calcium is not bound at physiologic calcium concentration (2 mM). Furthermore, our data showed that "B:b" interactions were normal in the rfD-γE132A+GH structure and that polymerization was normal at 10 mM calcium. Thus, we conclude normal polymerization requires calcium bound at the β2-site in fibrinogen before the initiation of "B:b" interactions. As a result, with γE132A fibrinogen, when the bound calcium was lost at ≤1mM calcium, lateral aggregation was enhanced. We rationalized the increase in lateral aggregation and fiber thickness with a model that includes calcium-dependent conformational changes that occur concomitant with the "B:b" interaction, as previously described (*19*).

Previous X-ray crystal structures of fibrinogen fragment D showed that the side chain carboxylate of BβAsp398 coordinates calcium in the β2 calcium-binding site in native fragment D and shifts to interact with GHRPam when it is bound in the "b" polymerization site (*18, 19*). Furthermore, we found loss of calcium in the β2-site in the presence of GHRPam (*19*). As shown in the preceding manuscript, when aspartic acid at Bβ398 is substituted with alanine, both calcium binding at the β2-site and GHRP binding at "b" polymerization site were eliminated. Together these losses resulted in impaired polymerization. In contrast, the binding

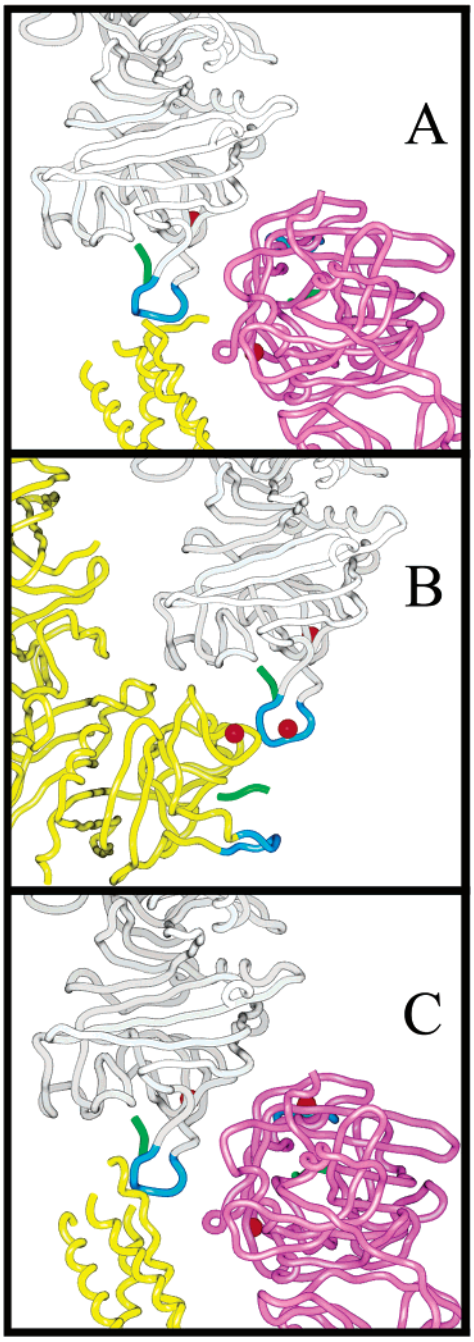

FIGURE 6: Crystal packing differences in structures rfD-BβD398A+GH and rfD-γE132A+GH. Panel A shows the packing interactions of one molecule of the asymmetric unit (gray) in the rfD-γE132A+GH structure with two symmetry-related molecules (yellow and pink). Note in this panel that calcium is not bound in the γ2-site (loop γ294−γ301, blue) even though GHRPam (green) is bound to the "a" polymerization site. Panel B depicts one molecule in the asymmetric unit in the rfD-BβD398A+GH structure (gray). Note that the symmetry-related molecule (yellow) is positioned in a different orientation than that in panel A or C and this orientation is associated with calcium bound (red sphere) in the γ2-site (blue) and GHRPam bound in the "a" polymerization site (green). Panel C shows the other molecule in the asymmetric unit in the rfD-BβD398A+GH structure (gray). Symmetry-related molecules (yellow and pink) are shown. Note their packing is similar to the packing shown in panel A. Also notice that GHRPam (green) is bound in the "a" polymerization site of these molecules but calcium is not bound to the γ2-site (blue). The second molecule in the asymmetric unit of the rfD-γE132A+GH and its packing interactions are not shown explicitly; however, they resemble the interactions in panel C.

of GHRPam was not impaired but calcium affinity to the β2-site was weakened in γE132A fibrinogen. Thus, at 10 mM calcium, polymerization is normal, while at $\leq$1 mM calcium, lateral aggregation was enhanced. This calcium dependency is the reverse of the well-established effect of calcium on polymerization with normal fibrinogen, where increasing calcium results in accelerated polymerization (*33*).

To explain such unusual behavior of γE132A fibrinogen, we propose that the β2 calcium-binding site together with the "B:b" interaction acts as a mechanism controlling lateral aggregation. In the fibrinogen conformation, BβAsp398 participates in the β2-site as a calcium-coordinating ligand. In the fibrin conformation, BβAsp398 undergoes a conformational flip to interact with the "B" sequence, GHRP. As a result of this flip, the β2 calcium-binding site is eliminated leading to disengagement of the β-module from the coiled coil connector. Thus, during polymerization, the "b" polymerization site and β2 calcium-binding site are in direct competition for residue Bβ398. Since the β2-site is impaired in γE132A fibrinogen, this competition is absent, which lowers the energy barrier for establishing the "B:b" interaction. We infer that by eliminating the β2 calcium-binding site we have increased the rate of lateral aggregation in γE132A fibrin by allowing "B:b" interactions to happen more efficiently. In further support of the β2 calcium-binding site's role, previous experiments showed that high calcium concentrations (>20 mM) have a negative impact on lateral aggregation and fiber thickness (*34*; Gorkun, unpublished observations). This fact is consistent with the proposed mechanism because at high concentrations calcium will remain bound to the β2-site, thus hindering the ability of residue Bβ398 to flip to its "fibrin conformation" resulting in delay of the "B:b" interaction.

Although such unusual calcium dependence of fibrin polymerization has never been reported experimentally, similar polymerization curves were produced in a model proposed by Weisel and Nagaswami (*35*). In this model, polymerization profiles similar to the polymerization profiles with γE132A fibrin were obtained when the rate at which two protofibrils aggregate to initiate a fiber was lower or the rate at which protofibrils join the growing fiber was higher compared to normal. Our data cannot discriminate which rate constant was changed in γE132A fibrinogen because we did not study the kinetics of protofibril formation. Nevertheless, the model profiles indicate that the γE132A substitution altered the kinetics of the assembly of protofibrils into fibers.

Enhanced "B:b" interactions are not the only event affecting γE132A fibrin polymerization. We have proposed previously that the β2 calcium-binding site functions as an anchor between the β-module and the coiled coil connector of the fibrinogen molecule. When the anchor is eliminated during the course of normal polymerization, the β-module gains freedom to move. Since the β2-site is absent in γE132A fibrinogen, there is no anchor, and thus, the β-module may possess an increased mobility very early in the polymerization reaction. Abolition of both the anchor and the "B:b" interaction leads to impaired thrombin-catalyzed polymerization (as in BβD398A fibrinogen polymerization, preceding manuscript). When the "B:b" interaction is disrupted and not the anchor as with BβE397A fibrinogen, polymerization is impaired again (preceding manuscript). In contrast to these

variants, γE132A fibrinogen, which only possesses a disrupted calcium anchor without impairment of "B:b" interactions, exhibits enhanced thrombin-catalyzed polymerization at physiological calcium concentrations.

A result of our experiments was the discovery that the structure of rfD-γE132A+GH did not possess a bound calcium ion in the γ2-site as previously observed with other fragment D crystals in the presence of GHRPam (*18*) (preceding manuscript). We believe this discrepancy indicates that the γ2 calcium-binding site in loop γ294−γ301 is a result of crystal-packing interactions, only coincidental to GHRPam binding to the "a" polymerization site as previously suggested (*18*). This conclusion was reached by considering two basic points. As mentioned in the preceding manuscript, the rfD-Bβ D398A+GH structure revealed only one molecule in the asymmetric unit exhibiting calcium bound to the γ2-site. The asymmetry in the appearance of the γ2-site in the rfD-Bβ D398A+GH structure suggested that the site was induced by crystal-packing interactions. Furthermore, the rfD-γE132A+GH structural data confirms the γ2-site to be crystal-packing-induced because the rfD-γE132A+GH crystal (1) has different unit cell dimensions than the rfD-Bβ D398A+GH structure, meaning molecules are packed differently and (2) shows no calcium bound at the γ2-site in either of the two molecules in the asymmetric unit of the crystal even though GHRPam is bound in the "a" polymerization site of both molecules. Detailed analysis of molecular contacts in the rfD-Bβ D398A+GH structure revealed the critical packing interaction that occurs to induce the γ2-site. Specifically, the backbone nitrogen of residue γAsp297 of one molecule in the asymmetric unit interacts with the backbone carbonyl of residue γAsn361 of a molecule in another asymmetric unit. The interaction results in the flip of the backbone carbonyl of residue γGly296 (next to the interacting γAsp297) to become a calcium ligand in the γ2-site. This particular contact is only seen in one molecule in the asymmetric unit of the rfD-Bβ D398A+GH structure, Figure 6B.

To rationalize the phenomena of crystal-packing-induced calcium binding in fibrinogen fragment D, we propose two hypotheses. We can consider the packing-induced calcium binding an artificial event taking place only in the crystal and not normally present in the fibrinogen or fibrin molecule. On the other hand, the ability of the protein to produce a calcium-binding site due to contact with another molecule can represent an unknown mechanism by which fibrin molecules are linked together in a fibrin polymer. The exact orientation and molecular contacts of fibrin molecules in the fibrin polymer are unknown. Thus, one can imagine that upon contacts of fibrin molecules in the polymer new calcium-binding sites are induced. These sites can act as calcium bridges between molecules, or they can play an important role in maintaining a "polymer conformation" of the fibrin molecule, or both. This mechanism is consistent with the observed calcium uptake associated with fibrinopeptide B release and subsequent lateral aggregation (*36*).

In summary, we have shown biochemical and X-ray crystal data for a variant fibrinogen, γE132A, that was designed to disrupt the β2 calcium-binding site. The data clearly show that the early disruption of the β2-site neighboring the "b" polymerization site positively influences fibrin polymerization in vitro. The data also show polymerization of the variant γE132A can be returned to normal at 10 mM calcium chloride, presumably by induced occupation of the β2 calcium-binding site. The structural data reported here and previously demonstrate that site-directed mutagenesis of fibrinogen can target specific interactions with little consequence to local or global structure. In addition, our data allowed us to shed light on the appearance of the γ2 calcium-binding site in loop γ294−γ301, which we demonstrated arises from crystal-packing interactions.

ACKNOWLEDGMENT

We thank Dr. Matthew R. Redinbo (UNC-CH, Chapel Hill, NC) for his guidance throughout this project and for sharing synchrotron time. We thank Dr. David K. Worthylake and members of Dr. John Sondek's laboratory (UNC-CH, Chapel Hill, NC) for their helpful discussions. We thank Dr. Laurie Betts for her technical suggestions, Dr. Brenda Temple at the UNC-CH Structural BioInformatics Core Facility (Chapel Hill, NC) for use of the computing facilities, the National Cell Culture Center for providing normal recombinant fibrinogen medium, and Stanford Synchrotron Radiation Laboratory for beamtime. We also thank Dr. Betsy Merenbloom for critical comments on this manuscript.

NOTE ADDED AFTER ASAP POSTING

This article was released ASAP on 2/10/2004. Subsequently, a change was made to ref 31, and the article was reposted on 2/12/2004.

REFERENCES

1. Doolittle, R. F. (1984) *Annu. Rev. Biochem. 53*, 195−229.
2. Brown, J. H., Volkmann, N., Jun, G., Henschen-Edman, A. H., and Cohen, C. (2000) *Proc. Natl. Acad. Sci. U.S.A. 97*, 85−90.
3. Doolittle, R. F., Goldbaum, D. M., and Doolittle, L. R. (1978) *J. Mol. Biol. 120*, 311−325.
4. Weisel, J. W., Stauffacher, C. V., Bullitt, E., and Cohen, C. (1985) *Science 230*, 1388−1391.
5. Olexa, S. A., and Budzynski, A. Z. (1980) *Proc. Natl. Acad. Sci. U.S.A. 77*, 1374−1378.
6. Laudano, A. P., and Doolittle, R. F. (1980) *Biochemistry 19*, 1013−1019.
7. Laudano, A. P., Cottrell, B. A., and Doolittle, R. F. (1983) *Ann. N. Y. Acad. Sci. 408*, 315−329.
8. Everse, S. J., Spraggon, G., Veerapandian, L., Riley, M., and Doolittle, R. F. (1998) *Biochemistry 37*, 8637−8642.
9. Hantgan, R., McDonagh, J., and Hermans, J. (1983) *Ann. N. Y. Acad. Sci. 408*, 344−366.
10. Weisel, J. W., Veklich, Y., and Gorkun, O. (1993) *J. Mol. Biol. 232*, 285−297.
11. Furlan, M., Seelich, T., and Beck, E. A. (1976) *Thromb. Haemostasis 36*, 582−592.
12. Lounes, K. C., Ping, L., Gorkun, O. V., and Lord, S. T. (2002) *Biochemistry 41*, 5291−5299.
13. Boyer, M. H., Shainoff, J. R., and Ratnoff, O. D. (1972) *Blood 39*, 382−387.
14. Cooke, R. D. (1974) *Biochem. J. 141*, 683−691.
15. Dang, C. V., Bell, W. R., Ebert, R. F., and Starksen, N. F. (1985) *Arch. Biochem. Biophys. 238*, 452−457.
16. Yee, V. C., Pratt, K. P., Cote, H. C., Trong, I. L., Chung, D. W., Davie, E. W., Stenkamp, R. E., and Teller, D. C. (1997) *Structure 5*, 125−138.
17. Spraggon, G., Everse, S. J., and Doolittle, R. F. (1997) *Nature 389*, 455−462.
18. Everse, S. J., Spraggon, G., Veerapandian, L., and Doolittle, R. F. (1999) *Biochemistry 38*, 2941−2946.
19. Kostelansky, M. S., Betts, L., Gorkun, O. V., and Lord, S. T. (2002) *Biochemistry 41*, 12124−12132.
20. Binnie, C. G., Hettasch, J. M., Strickland, E., and Lord, S. T. (1993) *Biochemistry 32*, 107−113.

21. Deng, W. P., and Nickoloff, J. A. (1992) *Anal. Biochem. 200*, 81−88.
22. Lord, S. T., Strickland, E., and Jayjock, E. (1996) *Biochemistry 35*, 2342−2348.
23. Gorkun, O. V., Veklich, Y. I., Weisel, J. W., and Lord, S. T. (1997) *Blood 89*, 4407−4414.
24. Ng, A. S., Lewis, S. D., and Shafer, J. A. (1993) *Methods Enzymol. 222*, 341−358.
25. Mullin, J. L., Gorkun, O. V., and Lord, S. T. (2000) *Biochemistry 39*, 9843−9849.
26. Furlan, M., Rupp, C., and Beck, E. A. (1983) *Biochim. Biophys. Acta 742*, 25−32.
27. Everse, S. J., Pelletier, H., and Doolittle, R. F. (1995) *Protein Sci. 4*, 1013−1016.
28. Otwinowski, Z. M. W. (1997) *Methods Enzymol. 276*, 307−326.
29. Brunger, A. T., Adams, P. D., Clore, G. M., DeLano, W. L., Gros, P., Grosse-Kunstleve, R. W., Jiang, J. S., Kuszewski, J., Nilges, M., Pannu, N. S., Read, R. J., Rice, L. M., Simonson, T., and Warren, G. L. (1998) *Acta Crystallogr., Sect. D 54*, 905−921.
30. Brunger, A. T. (1993) *Acta Crystallogr., Sect. D 49*, 24−36.
31. Jones, T. A., Zou, J. Y., Cowan, S. W., and Kjeldgaard, M. (1991) *Acta Crystallogr., Sect. A 47*, 110−119.
32. Read, R. J. (1986) *Acta Crystallogr., Sect. A 42*, 140−149.
33. Furlan, M., Rupp, C., Beck, E. A., and Svendsen, L. (1982) *Thromb. Haemostasis 47*, 118−121.
34. Carr, M. E., Jr. (1988) *Am. J. Med. Sci. 295*, 433−437.
35. Weisel, J. W., and Nagaswami, C. (1992) *Biophys. J. 63*, 111−128.
36. Mihalyi, E. (1988) *Biochemistry 27*, 967−976.

BI0359978